Journal of Robotic Systems, vol. 12, no. 10, October 1995, pp. 693-707.

A DYNAMIC COUPLING INDEX FOR UNDERACTUATED MANIPULATORS

Marcel Bergerman[†] Christopher Lee[‡] Yangsheng Xu[‡]

[†]Department of Electrical and Computer Engineering
[‡]The Robotics Institute
Carnegie Mellon University
5000 Forbes Avenue
Pittsburgh PA 15213

Journal of Robotic Systems, vol. 12, no. 10, October 1995, pp. 693-707.

Abstract

In recent years, researchers have been dedicated to the study of underactuated manipulators which have more joints than control actuators. In previous works, one always assumes that there is enough dynamic coupling between the active and the passive joints of the manipulator, for it to be possible to control the position of the passive joints via the dynamic coupling. In this work, the authors aim to develop an index to measure the dynamic coupling, so as to address when control of the underactuated system is possible, and how the motion and robot configuration can be designed. We discuss extensively the nature of the dynamic coupling and of the proposed coupling index, and their applications in the analysis and design of underactuated systems, through a detailed mathematical analysis and several illustrative examples.

1 Introduction

In recent years, researchers have been turning their attention to the so called underactuated systems, where the term *underactuated* refers to the fact that the system has more joints than control actuators. Some examples of underactuated systems are robot manipulators with failed actuators; free-floating space robots, where the base can be considered as a virtual passive linkage in inertia space; legged robots with passive joints; hyper-redundant (snake-like) robots with passive joints, etc.

These examples justify the importance of the study of underactuated systems. For example, if some actuators of a conventional manipulator fail, the loss of one or more degrees of freedom may compromise an entire operation. In free-floating space systems, the base (satellite) can be considered as a 6-DOF device without positioning actuators. Finally, manipulators with passive joints and hyper-redundant robots with few actuators are important from the viewpoint of energy saving, lightweight design and compactness.

Most of the results available in the literature for fully-actuated systems are difficult to apply to these new ones, because of the complications that appear in their dynamic formulation. Manipulators with passive joints present nonholonomic constraints, and the conditions for integrability of these constraints cannot be met in the general case.[9] The control system must cope with these constraints and hopefully take advantage of them to guarantee stability and performance requirements. Furthermore, as opposed to conventional manipulators, in this problem there is a guarantee that no smooth control law can achieve stability of the system to an equilibrium point.[7,9] Thus, one is left with the choice of procuring a discontinuous control law to reach a desired equilibrium position, or being content with controlling the system to an equilibrium manifold.

Recent works present control strategies to deal with the joint and Cartesian control problem of underactuated manipulators. Arai and Tachi[1] presented a method which requires brakes to be installed on each passive joints. The controller uses the dynamic coupling between the active and the passive joints in order to drive the passive joints to a desired set-point. Later, Bergerman and Xu[2] enhanced this method to deal with parameter uncertainty and provide the system with a greater deal of robustness. This is specially important in these systems because the Jacobian mapping from

Cartesian to joint space depends on the dynamic parameters, once again differently from conventional robots, where the Jacobian depends solely on kinematic parameters. Parameter uncertainty can lead the system to a very poor or even unstable performance. Another interesting control strategy requiring the use of brakes was demonstrated by Papadopoulos and Dubowsky,[10] this time for a space manipulator.

In every work mentioned above, the authors had to assume that “enough” coupling existed between the passive and the active joints, so that the controller could “transmit” the forces/torques to the passive joints in order to drive them. However, no attempts were made to quantify this coupling, or to identify the cases when it is too small as to be practically unfeasible to control the passive joints. To give the reader an introductory feeling of the importance of the dynamic coupling in underactuated mechanisms, consider a Cartesian 3-DOF manipulator, where the joint axes are mutually perpendicular. It can be verified that the inertia matrix for this manipulator is diagonal and constant, corresponding to the physical fact that there is no coupling at all between the joints. No matter how much one joint travels, the other ones are unaffected. Consequently, the absence of coupling does not allow this mechanism to be controlled at all if passive joints are present.

In this work, the authors aim to provide a measure of the dynamic coupling present in underactuated systems. This measure is useful not only for the design of an underactuated manipulator, so as to maximize the coupling and hopefully minimize the energy necessary to perform control; it is also useful for such important issues as actuator placement and control strategies. We present in the following sections the derivation of such coupling measure, and illustrate each concept introduced with clarifying examples.

2 Dynamic Coupling

The nonholonomic constraints present in the dynamic equation of a manipulator with passive joints cannot be integrated in general. Even partial integrability of the acceleration relationships to velocity ones is not possible in most cases.[9] This restriction makes it impossible to obtain a direct relationship between the angles of the passive joints and that of the active ones. Thus, it is necessary to work with the dynamic equations in their original form, and to try to derive acceleration relationships to quantify the dynamic coupling.

In order to derive the measure of dynamic coupling between the accelerations of the passive and active joints of an underactuated manipulator, we must first present the dynamic equations governing the behavior of the system. Let n be the total number of joints, r the number of active joints, and $p = n - r$ the number of passive ones. By using the Lagrangian formulation[3] one can obtain the following set of differential equations relating the accelerations of the joints to the torques supplied by the actuators:

$$M_0(q_0)\,\ddot{q}_0 + b_0(q_0, \dot{q}_0) = \tau_0 \tag{1}$$

Here, the matrix M_0 is the $n \times n$ inertia matrix of the manipulator, b_0 is a vector containing all the centrifugal, Coriolis and gravitational torques, and τ_0 is the vector of torques applied at the active joints. Note that τ_0 has always p components equal to zero, corresponding to the absence of actuators at the passive joints.

Since equation (1) does not reveal the relationship between the active and the passive joints' accelerations, we rearrange it as:

$$\begin{matrix} r \\ p \end{matrix} \begin{bmatrix} M_{aa} & M_{ap} \\ M_{pa} & M_{pp} \end{bmatrix} \begin{bmatrix} \ddot{q}_a \\ \ddot{q}_p \end{bmatrix} + \begin{bmatrix} b_a \\ b_p \end{bmatrix} = \begin{bmatrix} \tau_a \\ 0 \end{bmatrix} \tag{2}$$
$$\begin{matrix} & r & p \end{matrix}$$

where q_a corresponds to the active joint angles, q_p to the passive ones, and $q = [q_a{}^T \; q_p{}^T]^T$. It must be noted that M as defined in (2) *is not always equal* to the conventional inertia matrix of mechanical manipulators. Nonetheless, M still preserves important properties of the original inertia matrix, such as symmetry and positive-definiteness, as demonstrated in the Appendix.

The submatrices of M in (2) receive their indices according to the variables they relate. For example, M_{pa} relates the (null) torques at the passive joints to the acceleration of the active ones. The same reasoning is true for the other three submatrices. From the second line of (2), we can write:

$$M_{pa}\ddot{q}_a + M_{pp}\ddot{q}_p + b_p = 0 \tag{3}$$

and, since M_{pp} is positive-definite (see Appendix):

$$\ddot{q}_p = -M_{pp}^{-1} M_{pa} \ddot{q}_a - M_{pp}^{-1} b_p \tag{4}$$

The second term on the right-hand side of (4) is a function only of q and $\dot{q}$, and as such is completely determined once measurements of these variables are available. Because we are focusing on the acceleration relationship between the active and the passive joints, we rewrite equation (4) as:

$$\begin{aligned} \ddot{\bar{q}}_p &= -M_{pp}^{-1} M_{pa} \ddot{q}_a \\ &\equiv M_c \ddot{q}_a \end{aligned} \tag{5}$$

where

$$\ddot{\bar{q}}_p = \ddot{q}_p + M_{pp}^{-1} b_p \tag{6}$$

The acceleration $\ddot{\bar{q}}_p$ can be viewed as a virtual acceleration of the passive joints, generated by the acceleration of the active ones, and by the nonlinear torques due to velocity effects.

Equation (5) is important in the understanding of how an underactuated system works. Torques can only be applied at those joints which contain an actuator, or the active joints. These torques produce the accelerations $\ddot{q}_a$, which indirectly produce the accelerations $\ddot{q}_p$ at the passive joints. The passive joints' accelerations can only be controlled if the $p \times r$ matrix M_c possesses a structure that allows the actuators torques to be transmitted reasonably "well" (in a sense to be defined later) to the passive joints. Thus, the study of this matrix is of fundamental importance for the design and control of underactuated manipulators.

To begin the analysis, note that matrix M_c is a function only of the robot's configuration *q*, and thus is completely determined based on the readings of the encoders in all joints. It does not depend on $\ddot{q}_a$ or $\ddot{q}_p$. Thus, equation (5) can be regarded as a linear system of p equations $Ax = b$, underconstrained for $r > p$ and overconstrained for $r < p$. One result that can be immediately derived from the structure of (5) is:

Proposition 1 If row i, $1 \le i \le p$, in matrix M_c contains only zeros, then the i-th passive joint cannot be controlled via the dynamic coupling with the active joints.

This propositions follows from the fact that, if M_c has a line of zeros, then the i-th line in equation (4) reduces to:

$$\ddot{q}_{p_i} = \left(-M_{pp}^{-1} b_p \right)_i \tag{7}$$

This equality indicates that the acceleration of the i-th passive joint is not a function of any of the active joints' accelerations, and thus cannot be controlled directly.

Example 1 Consider a simple two-link manipulator as shown in Figure 1. Joint 1 rotates around the Z axis, while joint 2 rotates around an axis perpendicular to the first joint axis. The inertia matrix M_0 for this system is:

$$M_0 = \begin{bmatrix} m_2 l_{c_2}^2 \sin(\theta_2)^2 + I_1 + I_2 & 0 \\ 0 & m_2 l_{c_2}^2 + I_2 \end{bmatrix} \tag{8}$$

where m_2 is the mass of link 2, I_i are the inertias of links i = 1, 2, and l_{c_2} is the distance between joint 2 and the center of gravity of link 2. Two cases can be considered here: either joint 1 is active and joint 2 is passive, or vice-versa. For the first case, we have:

$$M_{pa} = 0, \qquad M_{pp} = m_2 l_{c_2}^2 + I_2 \tag{9}$$

and therefore:

$$M_c = 0 \tag{10}$$

Equation (9) indicates that it is not possible to control $\ddot{q}_2$ via its coupling with $\ddot{q}_1$. Thus, this underactuated system would not be useful for practical purposes. In the case for which joint 1 is passive, the result is the same:

$$M_{pa} = 0, \qquad M_{pp} = m_2 l_{c_2}^2 \sin(\theta_2)^2 + I_1 + I_2 \tag{11}$$

$$M_c = 0 \tag{12}$$

We can conclude that this mechanism's structure does not allow its passive joint to be controlled through the coupling with the active one, whether the active joint is joint 1 or 2. Note that this statement *does not imply that* the joints do not have any coupling at all. In fact, the second term in the right-hand side of (4) is generally non-zero, and so the passive joint may be disturbed for a given motion of the active one. However, the acceleration of the passive joint due to the coupling is non-controllable. ■

Example 2 Consider now the 2-link planar manipulator shown in Figure 2. For this system, we have:

$$M = \begin{bmatrix} m_1 l_{c_1}^2 + m_2\left[l_1^2 + l_{c_2}^2 + 2 l_1 l_{c_2}\cos(\theta_2)\right] + I_1 + I_2 & m_2\left[l_{c_2}^2 + l_1 l_{c_2}\cos(\theta_2)\right] + I_2 \\ m_2\left[l_{c_2}^2 + l_1 l_{c_2}\cos(\theta_2)\right] + I_2 & m_2 l_{c_2}^2 + I_2 \end{bmatrix} \tag{13}$$

Considering joint 1 active, and joint 2 passive, we have:

$$M_{pa} = m_2\left[l_{c_2}^2 + l_1 l_{c_2}\cos(\theta_2)\right] + I_2, \qquad M_{pp} = m_2 l_{c_2}^2 + I_2 \tag{14}$$

$$M_c = -\left[1 + \frac{m_2 l_1 l_{c_2}\cos(\theta_2)}{m_2 l_{c_2}^2 + I_2}\right] \tag{15}$$

Note that for this mechanism the structure does not prevent torque from being transmitted from the active to the passive joint, as it was the case in example 1. A numerical characterization of this transmission will be given in section 3. ■

3 Dynamic Coupling Measure

Since the submatrix M_{pp} in (2) is invertible, we can study the relationship (5) between the accelerations of the passive and active joints. According to our definition, M_c is a $p \times r$ matrix. We must study the various possibilities that can arise depending on whether there are more active or more passive joints in the mechanism. The first consideration that can be made regards the rank of matrix M_c. It is known that this rank obeys:

$$\text{rank}\,(M_c) \leq \min\,(p, r) \tag{16}$$

This fact will be used in the sequence.

• Case 1: $r < p$

Although this may not be common, it may happen that the number of actuators is smaller than the number of passive joints (e.g., when two actuators of a 3-DOF arm fail). In this case, M_c has maximum rank *r*, and equation (5) has *at most* one solution. However, this solution (if it exists) is not interesting in practice, because the accelerations of $p - r$ passive joints will depend linearly on the accelerations of the other *r* passive joints. In other words, *r* passive joints can be controlled at every instant, while the other $p - r$ of them cannot. We can conclude that it is necessary to have *at least p* actuators in the underactuated mechanism to be possible to control all *p* passive joints independently. Note that this result was already established by Arai and Tachi;[1] in their work, however, the authors reached this conclusion only after a study of the linearized dynamic equations of the system, while here we consider the nonlinearities present in the inertia matrix.

• Case 2: $r = p$

In this case we can obtain at most one solution, which exists if the $r \times r$ matrix M_c is invertible (or, in other words, if the submatrix M_{pa} is invertible). A case-by-case pre-analysis of M_c can show whether it will be possible to control $\ddot{q}_p$ using the actuators at the active joints.

• Case 3: $r > p$

This is probably the most common case, and certainly the most interesting one. Here, we can obtain *at least* one solution for the problem of finding the $\ddot{q}_a$ that will generate the desired $\ddot{q}_p$, provided the rank of matrix M_c is at least equal to p. In the general case, infinite solutions can be found. One can effectively make use of this redundancy to accomplish tasks such as obstacle avoidance, actuability maximization,[6] etc.

In any of the cases above, it is useful to define a measure of the dynamic coupling at any given instant. For example, when dealing with case 3, we can try to maximize the coupling via the use of the redundancy present in the system. Following Lee and Xu[6] and Xu and Shum,[11] it is natural to think of the singular values of M_c, which quantify its "degree of invertibility" and thus its capacity to "transmit" the torque from the active to the passive joints. Based on this, let $\sigma_1 \geq \sigma_2 \geq \ldots \geq \sigma_c$ be the $c = \min(p, r)$ singular values of M_c. We define the *coupling index* of the underactuated manipulator as:

$$\rho_c = \prod_{i=1}^{c} \sigma_i \tag{17}$$

As will be shown in the sequence, the coupling index can be used as a design tool for actuator placement, desirable robot configuration, or as a quantity to be used on the real-time control of the manipulator.

Example 3 Let's retake example 2, and apply the coupling index concept to it. The matrix M_c in this case is given by (15) and, since it is a scalar, we have:

$$\rho_c = \left| 1 + \frac{m_2 l_1 l_{c_2} \cos(\theta_2)}{m_2 l_{c_2}^2 + I_2} \right| \tag{18}$$

Let's adopt the following parameters for the quantities above: $m_2 = 1$ Kg, $l_1 = 0.3$ m, $l_{c_2} = 0.15$ m, $I_2 = 0.1$ Kg m^2. Then:

$$\rho_c = \left| 1 + 0.37 \cos\theta_2 \right| \tag{19}$$

We see that, for this manipulator, the matrix M_c is *always* invertible, and thus control of the passive joint via the dynamic coupling is always possible. Based on the present study, one can now pre-analyze the system in order to determine whether or not control is possible, before making any attempt to control it. ■

4 Manipulator Design

The coupling index can be used effectively on the design of the underactuated system as a mathematical tool that determines the optimal actuator placement of an underactuated manipulator. In the following we will use a series of examples to illustrate its importance.

Example 4 If we consider the same manipulator as in example 3, but now with joint 1 as the passive joint, we have the following results (the bars over the matrices were added so as to avoid confusion with the previous example):

$$\begin{aligned} \overline{M}_{pa} &= m_2\left[l_{c_2}^2 + l_1 l_{c_2}\cos(\theta_2)\right] + I_2 \\ \overline{M}_{pp} &= m_1 l_{c_1}^2 + m_2\left[l_1^2 + l_{c_2}^2 + 2l_1 l_{c_2}\cos(\theta_2)\right] + I_1 + I_2 \end{aligned} \tag{20}$$

Therefore:

$$\overline{M}_c = -\frac{m_2\left[l_{c_2}^2 + l_1 l_{c_2}\cos(\theta_2)\right] + I_2}{m_1 l_{c_1}^2 + m_2\left[l_1^2 + l_{c_2}^2 + 2l_1 l_{c_2}\cos(\theta_2)\right] + I_1 + I_2} \tag{21}$$

Substituting the values $m_1 = 2$ Kg, $I_1 = 0.2$ Kg m^2 in addition to the ones previously adopted, we obtain:

$$\bar{\rho}_c = \left|\frac{0.1225 + 0.045\cos\theta_2}{0.4575 + 0.090\cos\theta_2}\right| \tag{22}$$

Figure 3 shows how ρ_c and $\bar{\rho}_c$ vary as a function of θ_2. From this figure, we can infer that it is “easier” for joint 1 to drive joint 2 than vice-versa, because of the greater coupling available in

the average for the lower-actuated manipulator than that for the upper-actuated one. Thus, the coupling index indicates that, for the purpose of maximizing the dynamic coupling, joint 1 should be the active one, and joint 2 should be passive. ■

Note how this approach differs from the one studied by Lee and Xu,[6] where the authors define the *actuability index* of underactuated manipulators. The actuability index measures the arbitrariness of the actuator's ability to cause acceleration at the end-effector. Thus, *it relates torques in the active joints to accelerations at the end-effector in Cartesian space*, while the coupling index defined in this work *relates accelerations of the active joints to accelerations of the passive ones.* The conclusions derived in that work and the ones here should not be compared, for the indices operate in different manners. To be more specific, the coupling index indicates how much acceleration is possible to be obtained at the passive joints given limited accelerations at the active joints. There is no attempt to quantify the accelerations possible to be obtained at the end-effector. The actuability index indicates how much acceleration can be obtained at the end-effector given limited torques at the active joints. It does not attempt to quantify the accelerations at the passive joints.

In order to better provide the reader with an understanding of the difference between these two measures, we will briefly present the relationship of the acceleration of the end-effector to the torque at the active joint of the manipulator in example 4, for both upper- and lower-actuated cases. In the sequence, the subscripts *u* and *l* will be used to denote variables when the manipulator is, respectively, upper-actuated or lower-actuated.

The accelerations of the end-effector in *x* and *y* directions can be easily found to be:

$$\begin{aligned} \ddot{x} &= -\left[(l_1 c_1 + l_2 c_{12})\,\dot{\theta}_1^2 + 2 l_2 c_{12} \dot{\theta}_1 \dot{\theta}_2 + l_2 c_{12} \dot{\theta}_2^2 + (l_1 s_1 + l_2 s_{12})\,\ddot{\theta}_1 + l_2 s_{12} \ddot{\theta}_2 \right] \\ \ddot{y} &= -\left[(l_1 s_1 + l_2 s_{12})\,\dot{\theta}_1^2 + 2 l_2 s_{12} \dot{\theta}_1 \dot{\theta}_2 + l_2 s_{12} \dot{\theta}_2^2 - (l_1 c_1 + l_2 c_{12})\,\ddot{\theta}_1 - l_2 c_{12} \ddot{\theta}_2 \right] \end{aligned} \tag{23}$$

As before, we can consider the following virtual Cartesian accelerations, generated by the accelerations at the joints and the nonlinear effects:

$$\begin{aligned} \ddot{x} &= -\left[(l_1 s_1 + l_2 s_{12})\, \ddot{\theta}_1 + l_2 s_{12} \ddot{\theta}_2 \right] \\ \ddot{y} &= \left[(l_1 c_1 + l_2 c_{12})\, \ddot{\theta}_1 + l_2 c_{12} \ddot{\theta}_2 \right] \end{aligned} \tag{24}$$

Ignoring the nonlinear effects provenient from centrifugal, Coriolis and gravitational torques, we can write for the upper-actuated mechanism:

$$\begin{aligned} M_{2,1}\ddot{\theta}_1 + M_{2,2}\ddot{\theta}_2 &= 0 \quad \Rightarrow \quad \ddot{\theta}_2 = -(M_{2,1}/M_{2,2})\, \ddot{\theta}_1 \\ M_{1,1}\ddot{\theta}_1 + M_{1,2}\ddot{\theta}_2 &= \tau_u \quad \Rightarrow \quad \ddot{\theta}_1 = (M_{2,2}/\det(M))\, \tau_u \end{aligned} \tag{25}$$

where $M_{i,j}$ denotes the (*i*,*j*) element of the original inertia matrix M_0. Substituting (25) into (24) we obtain:

$$\begin{aligned} \ddot{x}_u &= -\left[l_1 s_1 + l_2 s_{12} \left(1 - \frac{M_{2,1}}{M_{2,2}} \right) \right] \frac{M_{2,2}}{\det(M_0)} \tau_u \\ \ddot{y}_u &= \left[l_1 c_1 + l_2 c_{12} \left(1 - \frac{M_{2,1}}{M_{2,2}} \right) \right] \frac{M_{2,2}}{\det(M_0)} \tau_u \end{aligned} \tag{26}$$

For the lower-actuated manipulator, the results are:

$$\begin{aligned} \ddot{x}_l &= -\left[-l_1 s_1 \left(\frac{M_{1,2}}{M_{1,1}} \right) + l_2 s_{12} \left(1 - \frac{M_{1,2}}{M_{1,1}} \right) \right] \frac{M_{1,1}}{\det(M_0)} \tau_l \\ \ddot{y}_l &= \left[-l_1 c_1 \left(\frac{M_{1,2}}{M_{1,1}} \right) + l_2 c_{12} \left(1 - \frac{M_{1,2}}{M_{1,1}} \right) \right] \frac{M_{1,1}}{\det(M_0)} \tau_l \end{aligned} \tag{27}$$

Figure 4 presents a comparison of the norm of the end-effector acceleration, $\|a\| = \left(\ddot{x}^2 + \ddot{y}^2 \right)^{1/2}$, which is a function of θ_2 only. The full line represents the upper-actuated mechanism, and the dashed line, the lower-actuated one. As we can see, the actuability of the upper-actuated mechanism is always greater than that of the lower-actuated one. This result contrasts with that represented by Figure 3, where we can see that the coupling index of the lower-actuated mechanism is always greater.

We illustrate the comments above with an example borrowed from Lee and Xu.[6] For the same manipulator, the actuability ellipsoid is shown in Figures 5 and 6, respectively for the lower- and the upper-actuated mechanism. As we can see, the actuability index, which is proportional to the volume (length, in this case) of the actuability ellipsoid, is greater for upper-actuated mechanisms. We refer the reader to Lee and Xu's work [6] for more detailed information on the actuability index.

Example 5 Let's consider now a "richer" example of a 3-DOF planar manipulator with rotary joints, as shown in Figure 7. The inertia matrix is given by:

$$M = \begin{bmatrix} M_{11} & M_{12} & M_{13} \\ M_{21} & M_{22} & M_{23} \\ M_{31} & M_{32} & M_{33} \end{bmatrix} \tag{28}$$

$$M_{11} = m_1 l_{c_1}^2 + m_2\left(l_1^2 + l_{c_2}^2 + 2l_1 l_{c_2} c_2\right) + m_3\left(l_1^2 + l_2^2 + l_{c_3}^2 + 2l_1 l_2 c_2 + 2l_1 l_{c_3} c_{23} + 2l_2 l_{c_3} c_3\right) + I_1 + I_2 + I_3$$

$$M_{12} = M_{21} = m_2\left(l_{c_2}^2 + l_1 l_{c_2} c_2\right) + m_3\left(l_2^2 + l_{c_3}^2 + l_1 l_2 c_2 + l_1 l_{c_3} c_{23} + 2l_2 l_{c_3} c_3\right) + I_2 + I_3$$

$$M_{13} = M_{31} = m_3\left(l_{c_3}^2 + l_1 l_{c_3} c_{23} + l_2 l_{c_3} c_3\right) + I_3$$

$$M_{22} = m_2 l_{c_2}^2 + m_3\left(l_2^2 + l_{c_3}^2 + 2l_2 l_{c_3} c_3\right) + I_2 + I_3$$

$$M_{23} = M_{32} = m_3\left(l_{c_3}^2 + l_2 l_{c_3} c_3\right) + I_3$$

$$M_{33} = m_3 l_{c_3}^2 + I_3$$

For simplicity, we adopt the same parameters as in example 4, and adopt for link 3 the same mass, length and inertia of link 2. We assume also that $r = 2$, i.e., we have two actuators to be placed either on joints 1 and 2, 1 and 3 or 2 and 3. In either case, M_c is a 1×2 matrix, what indicates that *at least* one solution to the problem of finding $\ddot{q}_a$ for a desired $\ddot{q}_p$ exists, provided that both elements of M_c are not equal to zero at the same instant (one such possible solution was demonstrated by Bergerman and Xu[2]). Let's compute the coupling index (here, the indices 1, 2 and 3 will be used to differentiate each case):

• Case 1: Joints 1 and 2 are active, joint 3 is passive

$$M_{c_1} = -\begin{bmatrix} 1 + 0.2727\,(c_{23} + c_3) & 1 + 0.2727 c_3 \end{bmatrix} \tag{29}$$

• Case 2: Joints 1 and 3 are active, joint 2 is passive

$$M_{c_2} = -\begin{bmatrix} \dfrac{0.3225 + 0.1350 c_2 + 0.030 c_{23} + 0.060 c_3}{0.3225 + 0.060 c_3} & \dfrac{0.1100 + 0.030 c_3}{0.3225 + 0.060 c_3} \end{bmatrix} \tag{30}$$

• Case 3: Joints 2 and 3 are active, joint 1 is passive

$$M_{c_3} = -\begin{bmatrix} \dfrac{0.3225 + 0.1350 c_2 + 0.030 c_{23} + 0.060 c_3}{0.7475 + 0.2700 c_2 + 0.060 c_{23} + 0.060 c_3} & \dfrac{0.1100 + 0.030 c_{23} + 0.030 c_3}{0.7475 + 0.2700 c_2 + 0.060 c_{23} + 0.060 c_3} \end{bmatrix} \tag{31}$$

Figures 8, 9 and 10 show the value of $\rho_{c_i}, i = 1, 2, 3$ as a function of both θ_2 and θ_3. A careful consideration of these figures shows that, for most values of the joint angles, ρ_{c_1} is the greatest index of all three. This can be verified by the values in Table 1. As we see, in none of the cases does ρ_{c_i} becomes zero (or "dangerously" close to zero). This indicates that at least one solution will always exist, no matter which joint is the passive one. Also, the choice of joint 3 as the passive joint increases the dynamic coupling, and enhances the control of the passive joint by the active ones. ■

5 Implementation Issues

5.1 Configuration Design

After going through the analysis in section 4, one can determine the best actuator placement so as to maximize the dynamic coupling between the active and the passive joints. One may also be interested on finding out the arm configurations that yield the maximum dynamic coupling for a given design of the manipulator and its workspace. Mathematically this corresponds to finding the joint angles *q* that maximize the coupling index. We will illustrate this concept with an example.

Example 6 Given the underactuated manipulator in Figure 2, let's suppose an actuator is placed at joint 1. As we saw, ρ_c is this case is given by (18). The joint angle θ_2 that maximizes that

expression can be found via:

$$\frac{d\rho_c}{d\theta_2} = -\frac{m_2 l_1 l_{c_2} \sin(\theta_2)}{m_2 l_{c_2}^2 + I_2} = 0 \tag{32}$$

or:

$$\theta_2 = 0 \tag{33}$$

(note that $\theta_2 = \pi$ corresponds to a point of minimum - see also Figure 3).

As we can see, the arm configuration that yields maximum dynamic coupling is the one where the arm is fully extended. Note how this differs from the results otherwise obtained when one considers the classical *manipulability measure*, introduced by Yoshikawa.[12] For a regular fully-actuated 2-DOF planar manipulator similar to the one treated in this example, this configuration yields the minimum of the manipulability measure. ■

5.2 Individual Joint Coupling

The coupling index, in addition to being useful on the design of the underactuated system, can also be used for real-time control. Bergerman and Xu[2] demonstrated the feasibility of driving a three-link planar manipulator with only two actuators located at joints 1 and 2. The passive joint (joint 3) and one active joint (joint 1) were controlled first. After the passive joint reached its set-point, it was locked, and then both active joints were controlled to their desired set-points. Although joint 1 was chosen to be controlled first, it may be the case that this joint has greater coupling with the passive joint than the other active one. If this were true, joint 1 should be used to drive the passive joint, and only be controlled after the passive joint is locked.

Basically, the idea is to define an *individual joint coupling index* relating each passive joint to each active one. Working with these pairs of active-passive joints, we can measure the dynamic coupling existent between each of them. Ultimately, our objective will be that of determining which active joint should be chosen to drive each passive one.

Recall equation (5); if we split it on its constituting lines, we have on line *i*:

$$\ddot{q}_{p_i} = M_{c_{i,1}} \ddot{q}_{a_1} + \ldots + M_{c_{i,r}} \ddot{q}_{a_r} \tag{34}$$

In order to study the coupling between the *i*-th passive and the *j*-th active joint, we can assign zero values to all except the *j*-th active joint's acceleration:

$$\ddot{q}_{p_i} = M_{c_{i,j}} \ddot{q}_{a_j} \tag{35}$$

This equation resembles (5) and so we can define the *coupling index between the i-th passive and the j-th active joint*:

$$\rho_{c_{ij}} = \left| M_{c_{i,j}} \right| \tag{36}$$

For every row in the matrix M_c, the element (i, j) with greater magnitude will indicate that the greatest dynamic coupling for the passive joint *i* comes from the active joint *j*.

Example 7 We will review the example presented Bergerman and Xu,[2] using the concept of individual joint coupling index defined above. The system under discussion is the one shown in Figure 7, where joints 1 and 2 are active and joint 3 is passive (according to the results in example 5). For this system, the matrix M_c is given by equation (30), which can also be read as:

$$\ddot{q}_{p_1} = -\left[1 + 0.2727\,(c_{23} + c_3)\right] \ddot{q}_{a_1} - \left[1 + 0.2727 c_3\right] \ddot{q}_{a_2} \tag{37}$$

According to (37) we have:

$$\begin{aligned} \rho_{c_{11}} &= \left|1 + 0.2727\,(c_{23} + c_3)\right| \\ \rho_{c_{12}} &= \left|1 + 0.2727 c_3\right| \end{aligned} \tag{38}$$

Table 2 presents the maximum, minimum, average and standard deviation values for $\rho_{c_{11}}$ and $\rho_{c_{12}}$. Based on these values, it is difficult to tell which active joint has greater coupling with the passive one. Although $\rho_{c_{11}}$ attains greater values than $\rho_{c_{12}}$, it also attains smaller values; and the

averages of both indices are the same. This example shows that the coupling index, although useful, may not provide the control engineer with sufficient information to decide on which active joint should drive the passive one. Global indices, based on the integral of the coupling index, may be more useful in this case, as it will be shown in the sequence. ■

5.3 Global Coupling Index

The coupling index defined previously is a local measure; it measures the "amount" of dynamic coupling between the active and the passive joints at every point in the joint space. The greater the coupling index at a particular configuration of the manipulator, the easier for the active joints to drive the passive ones.

However, in design and path planning problems, one is more interested in the coupling index in a global sense, so as to measure the dynamic coupling existent within the workspace of the manipulator. In this case, a *global coupling index* is more useful, for it will measure the coupling between the joints at *all* points in the joint space. One possible way of defining a global coupling index is as follows:[4]

$$\rho_c^g = \frac{\int_\Theta \rho_c^2 d\Theta}{\int_\Theta d\Theta} \tag{39}$$

where the integrals above are taken over the entire joint space $\Theta \in \Re^n$ of the manipulator. The use of the squared value of the coupling index is inert because the coupling index is always non-negative; and this choice facilitates the problem of finding a closed-form solution of the integral in the numerator, because the singular values of a matrix A are equal to the positive square roots of the nonzero eigenvalues of $A^T A$.

This choice of the global coupling index will take into account not only the local coupling between the joints, but that available over the entire joint space, as the next examples show.

Example 8 We re-analyze example 5, where the objective was to determine the best actuator placement based on the dynamic coupling between the joints. There, the decision to place the

actuators on joints 1 and 2 was based on the maximum, minimum and average values of ρ_c for the various possible configurations. Here we can base this decision on a global index, which already takes into account all these quantities.

The unique singular value of a 1×2 matrix is computed easily as:

$$A = \begin{bmatrix} a_1 & a_2 \end{bmatrix} \Rightarrow \sigma = \left(a_1^2 + a_2^2 \right)^{1/2} \tag{40}$$

Comparing A above with the various M_{c_i}, $i = 1, 2, 3$, of example 5, we have:

$$\rho_{c_i}^g = \frac{\int_\Theta \left(a_1^2 + a_2^2 \right) d\Theta}{\int_\Theta d\Theta} \tag{41}$$

We considered in the following calculations that the joints can rotate freely around their respective axis from 0 to 2π. In cases where there are physical joint limits, this can be taken into account in the calculation of the integrals in (40). For cases 1, 2, and 3 studied in example 5, we have the results shown in Table 3. We can immediately conclude that case 1 is the one which provides greater dynamic coupling between the active and the passive joints in a global sense. Note that this is the same conclusion as the one drawn in example 5, reached in a much simpler way. ■

Example 9 The global coupling index can also be used in conjunction with the individual joint coupling index defined in section 5.2. The idea is to use the later instead of ρ_c in equation (40):

$$\rho_{c_{ij}}^g = \frac{\int_\Theta \rho_{c_{ij}}^2 d\Theta}{\int_\Theta d\Theta} \tag{42}$$

Calculating the above *global individual joint coupling index* for the manipulator in example 7, we have the results shown in Table 4. We can see that the global coupling between the first and second active joints and the passive joint is exactly the same. For control purposes, then, one can

choose either active joint to dynamically control the passive joint. Note that this conclusion was drawn immediately, as opposed to example 7, where no conclusion could be drawn. ■

Example 10 The coupling index can also be useful for the purpose of designing the links of an underactuated mechanism. Suppose in the manipulator of Figure 2, with joint 1 active, we have available the following parameters: $m_2 = 1\text{Kg}$, $I_2 = 0.1\text{Kg} \cdot \text{m}^2$, $l_1 = 1\text{m}$. Additionally, suppose we want to determine l_{c_2} so as to maximize the global coupling index ρ_c^g. In this case we have:

$$\rho_c^g = \frac{1 + 70l_{c_2}^2 + 100l_{c_2}^4}{1 + 20l_{c_2}^2 + 100l_{c_2}^4} \tag{43}$$

Figure 11 presents the global coupling index as a function of l_{c_2}. As we can see, for $l_{c_2} = 0.316\text{m}$, it attains the maximum value $\rho_c^g = 2.250$. This example shows how the global coupling index can be used for design issues other than actuator placement. ■

5.4 Alternative Coupling Indices

5.4.1 Condition number of the matrix M_c

As explained by Nakamura,[8] other indices derived from the singular values of M_c can be useful. One of them is the *condition number* κ_c of M_c, defined as the ratio of the greatest to the smallest singular values. The condition number is very useful in the analysis of the sensitivity of equation (5). Even in the cases where ρ_c is large enough to guarantee the existence of dynamic coupling, the condition number can indicate that the relative errors between the acceleration of the active and the passive joints is also too big. In these cases, amplified noise can disturb the performance of the mechanism.

We will perform here a brief sensitivity analysis of (5), and see how this can influence the use of the coupling index. It is known that the norms of the accelerations in (5) obey:

$$\frac{1}{\sigma_1} \leq \frac{\|\ddot{q}_a\|}{\|\ddot{q}_p\|} \leq \frac{1}{\sigma_c} \tag{44}$$

If noise is present in the system and exhibits itself in the form of an error $\Delta\ddot{q}_p$ on $\ddot{q}_p$, then the corresponding error $\Delta\ddot{q}_a$ on $\ddot{q}_a$ obeys:

$$\frac{1}{\sigma_1} \leq \frac{\left\|\Delta\ddot{q}_a\right\|}{\left\|\Delta\ddot{q}_p\right\|} \leq \frac{1}{\sigma_c} \tag{45}$$

From equations (45) and (46) we can conclude that the ratio of the relative errors obeys:

$$\frac{1}{\kappa_c} \leq \frac{\left\|\Delta\ddot{q}_a\right\| / \left\|\ddot{q}_a\right\|}{\left\|\Delta\ddot{q}_p\right\| / \left\|\ddot{q}_p\right\|} \leq \kappa_c \tag{46}$$

As we can see, the ratio of the relative errors is never smaller than the inverse of the condition number, and never larger than the condition number. If κ_c is too big, errors will easily “travel” along the mechanism making the control scheme more difficult and the performance worst. These ill-conditioned matrices M_c can render the control scheme useless, even in the cases where the dynamic coupling is quite big.

5.4.2 Relationship to actuators’ torques

Both the local and global coupling indices provide the designer and control engineer with a measure of the coupling available between the active and passive joints of an underactuated mechanism. Based on their definition, one can quantify how much acceleration is needed at the active joints to produce a desired acceleration at the passive ones. In some cases, however, one may be interested on the relationship between accelerations at the passive joints and other physical variables. For example, energy minimization requires study of the relationship to the torques at the actuators. Since acceleration in a complex nonlinear mechanism such as a manipulator is not necessarily proportional to torque (and, hence, energy consumption), we cannot claim directly that a high coupling index as defined previously implies low energy spending. In order to make this claim, we define an alternative coupling index in the following paragraphs.

Factoring $\ddot{q}_a$ in the first line of (2), we obtain:

$$\ddot{q}_a = M_{aa}^{-1}(\tau_a - M_{ap}\ddot{q}_p - b_a) \tag{47}$$

Substituting this result on the second line of (2), the following relationship between the acceleration of the passive joints and the torques applied at the active ones is obtained:

$$\ddot{q}_p = -W_{pp}M_{pa}M_{aa}^{-1}\tau_a + W_{pp}\left(M_{pa}M_{aa}^{-1}b_a - b_p\right) \tag{48}$$

where the $p \times p$ matrix W_{pp} is the inverse of the Schur complement of M_{aa} in M, shown in the Appendix to be positive definite:

$$W_{pp} = \left(M_{pp} - M_{pa}M_{aa}^{-1}M_{ap}\right)^{-1} \tag{49}$$

Since we are focusing on the relationship between the accelerations of the passive joints and the active joints' torques, we can rewrite equation (49) as:

$$\begin{aligned} \ddot{q}_p &= -W_{pp}M_{pa}M_{aa}^{-1}\tau_a \\ &\equiv M_i\tau_a \end{aligned} \tag{50}$$

where

$$\ddot{q}_p = \ddot{q}_p - W_{pp}\left(M_{pa}M_{aa}^{-1}b_a - b_p\right) \tag{51}$$

As before, the vector $\ddot{q}_p$ can be considered as a virtual acceleration of the passive joints, generated by the active torques and the nonlinear torques due to velocity and gravitational effects. We can then define the following coupling index:

$$\rho_i = \prod_{k=1}^{q} \sigma_k \tag{52}$$

where $\sigma_1, ..., \sigma_q$ are the $q = \min(p,r)$ singular values of M_i.

Naturally, this coupling index can also be computed globally over the entire workspace of the manipulator:

$$\rho_i^g = \frac{\int_\Theta \rho_i^2 d\Theta}{\int_\Theta d\Theta} \tag{53}$$

This coupling index will be useful for the solution of control and planning problems of underactuated manipulators when energy consumption is at a premium (for example, in space applications.) The authors are currently studying its application on the control of underactuated mechanisms where the number of actuators is less than the number of passive joints ($p > r$.) Briefly, the idea consists on grouping the passive joints in groups of r joints each, and controlling each group to its desired set-point only after the previous one converged and is locked. After all groups of passive joints are controlled, the active ones can be controlled to their set-points. Because there are $\binom{p}{r}$ different ways of performing this grouping, we make use of dynamic programming techniques to ensure a global optimum solution to the joint control problem. The cost between phases of the control sequence is defined as the global coupling index (54), so that energy consumption can be indirectly minimized. Results on this work are expected to be published soon.

6 Conclusion

There has been considerable progress recently in the area of analysis and control of underactuated manipulators. The current literature in this area however, has always assumed that sufficient dynamic coupling was available between the active and passive joints for effective control of the manipulator. Because this assumption is not always valid, it is vital for design, analysis, and control of these systems that the amount of available coupling be quantified.

In this work, the authors propose a measure of the dynamic coupling between the active and passive joints of an underactuated manipulator. The coupling index indicates precisely the amount of coupling available for the purpose of controlling the passive joints of the manipulator through the application of torques in the active joints. We also propose a global coupling index, which indicates the amount of coupling available over the entire workspace of the manipulator.

As we show through a series of illustrative examples, the proposed indices can be used effectively within the contexts of mechanical design, configuration optimization, and real-time control.

7 Acknowledgments

We would like to acknowledge the fruitful discussions with Christiaan Paredis, Carnegie Mellon University, and Dr. Yasuyoshi Yokokohji, Visiting Research Scholar at Carnegie Mellon. The first author is supported by a grant from the Brazilian National Council for Research and Development (CNPq).

Appendix

In this appendix we show that the matrix M in (2) is symmetric and positive-definite. In addition, we show that the submatrices M_{pp} and W_{pp} are positive-definite. The first proof is based on the fact that M is obtained from M_0 after the swapping of rows and columns in an orderly fashion: if rows i and j are swapped, so must be columns i and j. Each swapping of rows and columns i and j can be described mathematically as:

$$M = T_{i,j} M_0 T_{i,j}^{-1} \tag{A.1}$$

where $T_{i,j}$ is a transformation matrix obtained from the identity matrix by the swapping of rows i and j (or columns i and j):

$$T_{i,j} = \begin{bmatrix} 1 & & & & & & \\ & 1 & & & & & \\ & & 0 & & 1 & & \\ & & & 1 & & & \\ & & 1 & & 0 & & \\ & & & & & 1 & \\ & & & & & & 1 \end{bmatrix} \begin{matrix} \\ \\ \leftarrow \text{row } i \\ \\ \leftarrow \text{row } j \\ \\ \end{matrix} \tag{A.2}$$

Equation (A.1) establishes that M and M_0 become *similar matrices* after one swapping operation. Naturally, this fact remains true after all swapping operations are performed. Now it is a known fact that the spectrum of similar matrices is the same,[5] and so we can conclude that the new inertia matrix of the manipulator, M, is positive definite.

Additionally, we can show that M is also symmetric. It is known that the original inertia matrix is symmetric, and that the transformation $T_{i,j}$ is symmetric and equal to its inverse. This allows us to write:

$$M^T = \left(T_{i,j} M_0 T_{i,j}^{-1} \right)^T = \left(T_{i,j}^{-1} \right)^T M_0^T T_{i,j}{}^T = T_{i,j} M_0 T_{i,j}^{-1} = M \tag{A.3}$$

and to conclude on the symmetry of M.

The $n \times n$ matrix M can be partitioned as in equation (2). Its elements are given by:

$$M = \left[\begin{array}{cccc|ccc} M_{1,1} & M_{1,2} & M_{1,3} & \cdots M_{1,r} & M_{1,r+1} & M_{1,r+2} & \cdots M_{1,n} \\ M_{2,1} & M_{2,2} & M_{2,3} & \cdots M_{2,r} & M_{2,r+1} & M_{2,r+2} & \cdots M_{2,n} \\ M_{3,1} & M_{3,2} & M_{3,3} & \cdots M_{3,r} & M_{3,r+1} & M_{3,r+2} & \cdots M_{3,n} \\ \cdots & \cdots & \cdots & \cdots \cdots & \cdots & \cdots & \cdots \cdots \\ M_{r,1} & M_{r,2} & M_{r,3} & \cdots M_{r,r} & M_{r,r+1} & M_{r,r+2} & \cdots M_{r,n} \\ \hline M_{r+1,1} & M_{r+1,2} & M_{r+1,3} & \cdots M_{r+1,r} & M_{r+1,r+1} & M_{r+1,r+2} & \cdots M_{r+1,n} \\ M_{r+2,1} & M_{r+2,2} & M_{r+2,3} & \cdots M_{r+2,r} & M_{r+2,r+1} & M_{r+2,r+2} & \cdots M_{r+2,n} \\ \cdots & \cdots & \cdots & \cdots \cdots & \cdots & \cdots & \cdots \cdots \\ M_{n,1} & M_{n,2} & M_{n,3} & \cdots M_{n,r} & M_{n,r+1} & M_{n,r+2} & \cdots M_{n,n} \end{array}\right] \tag{A.4}$$

It is possible to rearrange the rows and columns of M in order to move the submatrix M_{pp} to the upper left corner of M. For this purpose, one has to exchange rows and columns 1 and r+1, followed by rows and columns 2 and r+2, all the way to rows and columns n-r and n. This sequence of operations results in:

$$\hat{M} = \left[\begin{array}{ccc|ccccccccc} M_{r+1,r+1} & \cdots & M_{r+1,n} & M_{r+1,n-r+1} & M_{r+1,n-r+2} & \cdots & M_{r+1,r} & M_{r+1,1} & M_{r+1,2} & \cdots & M_{r+1,n-r} \\ \cdots & \cdots & \cdots & \cdots & \cdots & \cdots & \cdots & \cdots & \cdots & \cdots & \cdots \\ M_{n,r+1} & \cdots & M_{n,n} & M_{n,n-r+1} & M_{n,n-r+2} & \cdots & M_{n,r} & M_{n,1} & M_{n,2} & \cdots & M_{n,n-r} \\ \hline M_{n-r+1,r+1} & \cdots & M_{n-r+1,n} & M_{n-r+1,n-r+1} & M_{n-r+1,n-r+2} & \cdots & M_{n-r+1,r} & M_{n-r+1,1} & M_{n-r+1,2} & \cdots & M_{n-r+1,n-r} \\ M_{n-r+2,r+1} & \cdots & M_{n-r+2,n} & M_{n-r+2,n-r+1} & M_{n-r+2,n-r+2} & \cdots & M_{n-r+2,r} & M_{n-r+2,1} & M_{n-r+2,2} & \cdots & M_{n-r+2,n-r} \\ \cdots & \cdots & \cdots & \cdots & \cdots & \cdots & \cdots & \cdots & \cdots & \cdots & \cdots \\ M_{r,r+1} & \cdots & M_{r,n} & M_{r,n-r+1} & M_{r,n-r+2} & \cdots & M_{r,r} & M_{r,1} & M_{r,2} & \cdots & M_{r,n-r} \\ M_{1,r+1} & \cdots & M_{1,n} & M_{1,n-r+1} & M_{1,n-r+2} & \cdots & M_{1,r} & M_{1,1} & M_{1,2} & \cdots & M_{1,n-r} \\ \cdots & \cdots & \cdots & \cdots & \cdots & \cdots & \cdots & \cdots & \cdots & \cdots & \cdots \\ M_{n-r,r+1} & \cdots & M_{n-r,n} & M_{n-r,n-r+1} & M_{n-r,n-r+2} & \cdots & M_{n-r,r} & M_{n-r,1} & M_{n-r,2} & \cdots & M_{n-r,n-r} \end{array}\right]$$

This can also be described mathematically as:

$$\begin{aligned} \hat{M} &= T_{n-r,n}\cdots T_{2,r+2}T_{1,r+1}MT_{1,r+1}^{-1}T_{2,r+2}^{-1}\cdots T_{n-r,n}^{-1} = \\ \hat{M} &= \underbrace{(T_{n-r,n}\cdots T_{2,r+2}T_{1,r+1})}\ M\ \underbrace{(T_{n-r,n}\cdots T_{2,r+2}T_{1,r+1})^{-1}} = \\ \hat{M} &= \qquad\quad \hat{T} \qquad\qquad M \qquad\quad \hat{T}^{-1} \end{aligned} \tag{A.5}$$

The matrix $\hat{T}$ is an elementary matrix, for it is a product of elementary matrices. Thus $\hat{M}$ is similar to M and is, consequently, positive-definite. Now any upper square block of a positive-definite matrix is also positive-definite. Noting that the $p \times p$ upper block inside $\hat{M}$ is equal to M_{pp}, we get the desired result.

As for W_{pp}, we first note that if W is the inverse of the inertia matrix M, then W can be partitioned in the same manner as M:

$$W = \begin{bmatrix} W_{aa} & W_{ap} \\ W_{pa} & W_{pp} \end{bmatrix} \tag{A.6}$$

It can be verified that W_{pp} in (A.6) is given by equation (50). Note now that the relationship between W_{pp} and W is the same as that between M_{pp} and M; namely, W_{pp} is a diagonally-positioned square submatrix of a positive definite matrix. Following the steps used to prove that M_{pp} is positive definite, one can show that W_{pp} also possesses this property.

References

1. H. Arai and S. Tachi, "Position control of a manipulator with passive joints using dynamic coupling", *IEEE Transactions on Robotics and Automation*, vol. 7, no. 4, Aug. 1991, pp. 528-534.

2. M. Bergerman and Y. Xu, "Robust control of underactuated manipulators: analysis and implementation", *Proceedings of the IEEE Systems, Man and Cybernetics Conference*, Oct. 1994.

3. J. J. Craig, *Introduction to robotics*: Mechanics and control, Addison-Wesley, Reading, 2 ed., 1989.

4. C. Gosselin and J. Angeles, "A global performance index for the kinematic optimization of robotic manipulators", *Transactions of the ASME, Journal of Mechanical Design*, vol. 113, Sep. 1991, pp. 220-226.

5. P. Lancaster and M. Tismenetsky, *The theory of matrices,* Academic Press, Orlando, 2 ed., 1985, pp. 152.

6. C. Lee and Y. Xu, *Actuability of underactuated manipulators,* CMU-TR-RI-94-13, Carnegie Mellon University, May 1994. Submitted to the *1995 Conference on Control Applications.*

7. R. Mukherjee and D. Chen, "Control of free-flying underactuated space manipulators to equilibrium manifolds", *IEEE Transactions on Robotics and Automation*, vol. 9, no. 5, Oct. 1993.

8. Y. Nakamura, *Advanced robotics*: Redundancy and optimization, Addison-Wesley, Reading, 1ed., 1991.

9. G. Oriolo and Y. Nakamura, "Control of mechanical manipulators with second-order non-holonomic constraints: underactuated manipulators", *Proceedings of the 30th Conference on Decision and Control*, Dec. 1991, pp. 2398-2403.

10. E. Papadopoulos and S. Dubowsky, "Failure recovery control for space robotic systems", *Proceedings of the 1991 American Control Conference*, vol. 2, 1991, pp. 1485-1490.

11. Y. Xu and H. Y. Shum, "Dynamic control and coupling of free-floating space robot systems", to appear in *Journal of Robotic Systems.*

12. T. Yoshikawa, *Foundations of robotics*: Analysis and control, MIT Press, Cambridge, 1ed., 1990.

List of Figures

Figure 1: Two-link manipulator with rotary joints.

Figure 2: Two-link planar manipulator with rotary joints.

Figure 3: Coupling index between the joints of the robot in Figure 2.

Figure 4: End-effector acceleration for the mechanism in Figure 2.

Figure 5: Actuability index for the lower-actuated mechanism in Figure 2.

Figure 6: Actuability index for the upper-actuated mechanism in Figure 2.

Figure 7: Three-link planar manipulator with rotary joints.

Figure 8: Coupling index for the manipulator in Figure 7, when joint 3 is passive.

Figure 9: Coupling index for the manipulator in Figure 7, when joint 2 is passive.

Figure 10: Coupling index for the manipulator in Figure 7, when joint 1 is passive.

Figure 11: Global coupling index in example 11.

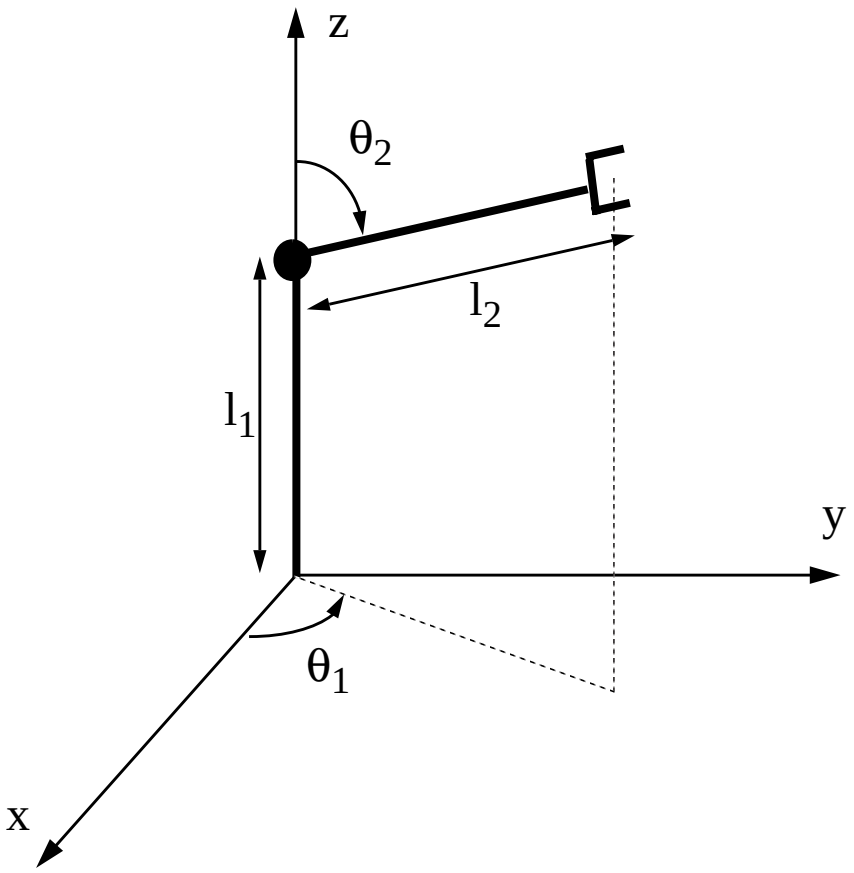


Figure 1: Two-link manipulator with rotary joints.

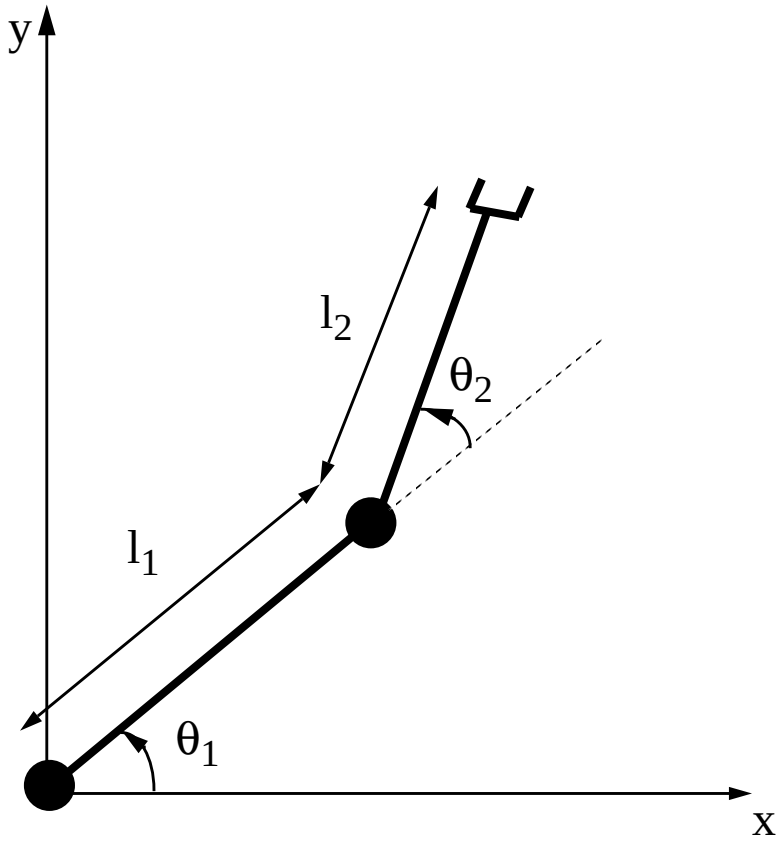


Figure 2: Two-link planar manipulator with rotary joints.

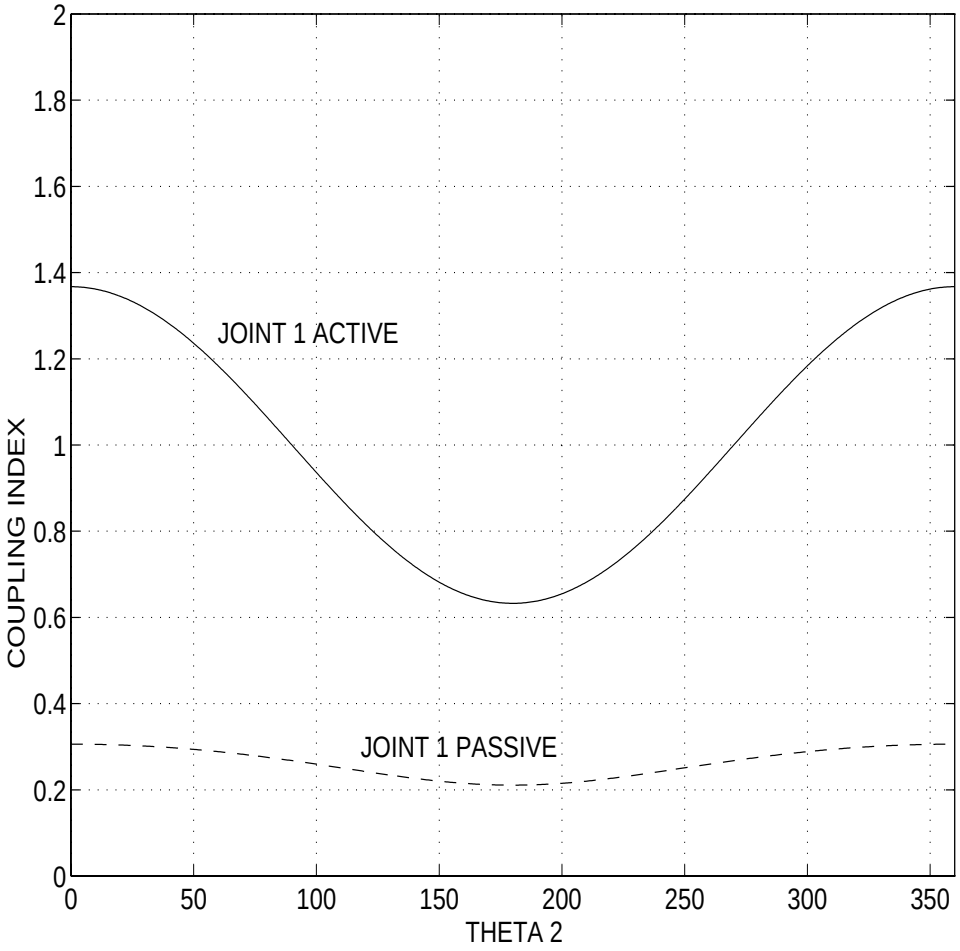


Figure 3: Coupling index between the joints of the robot in Figure 2.

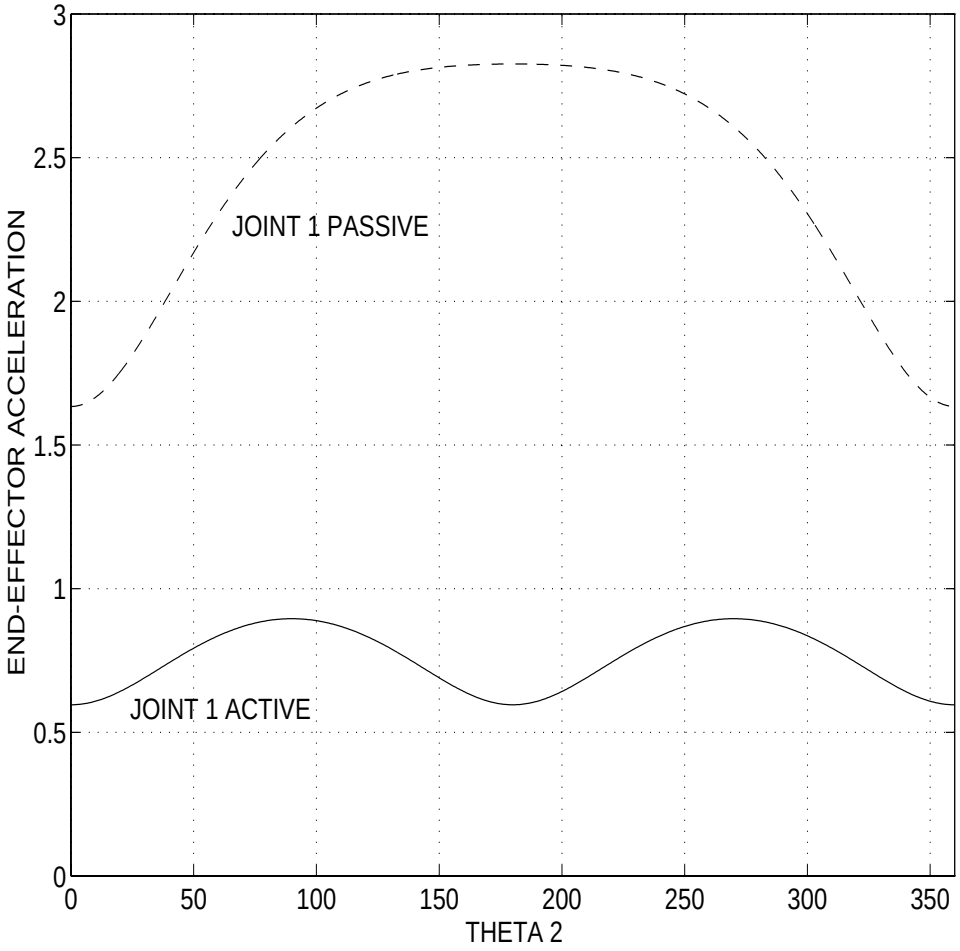


Figure 4: End-effector acceleration for the mechanism in Figure 2.

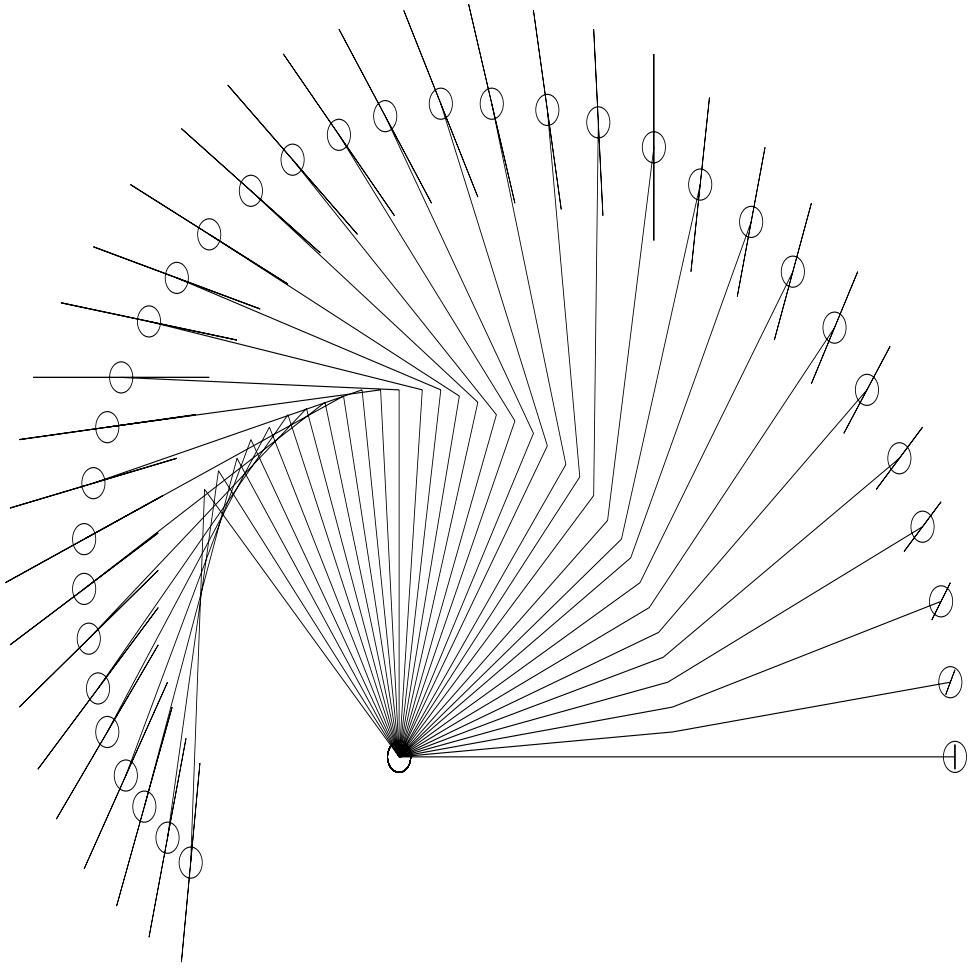


Figure 5: Actuability index for the lower-actuated mechanism in Figure 2.

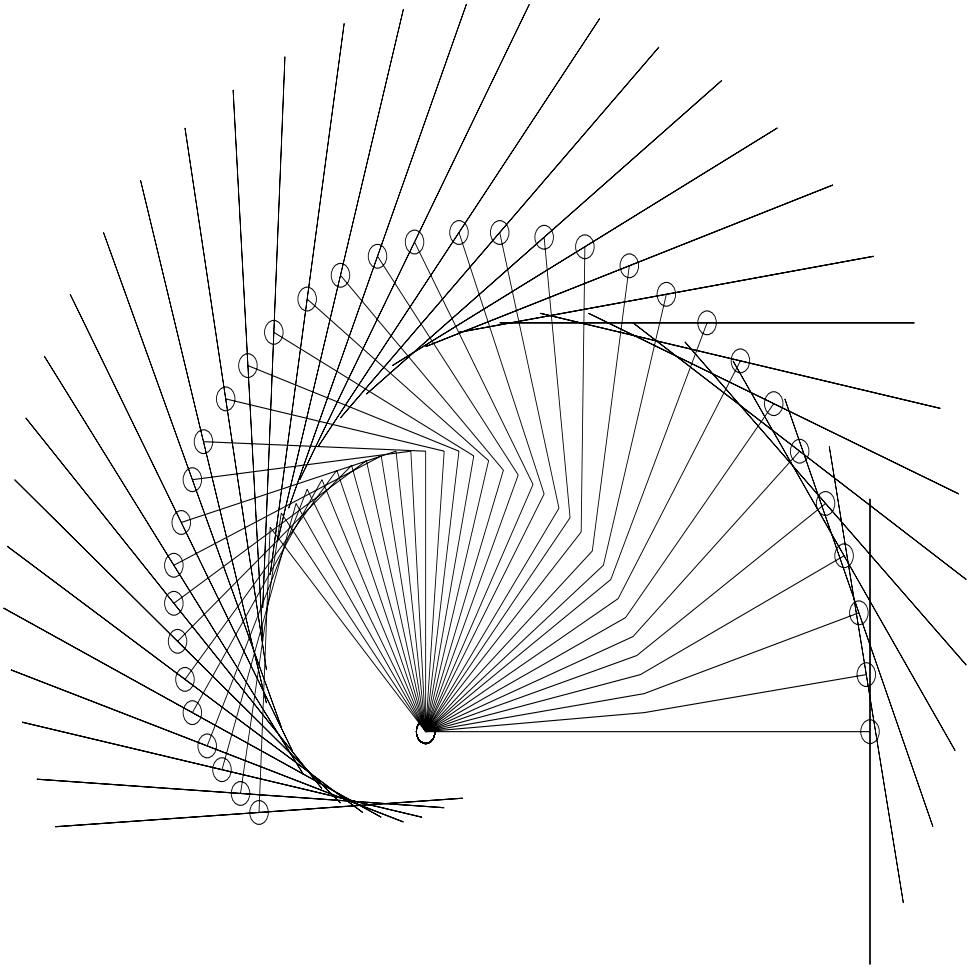


Figure 6: Actuability index for the upper-actuated mechanism in Figure 2.

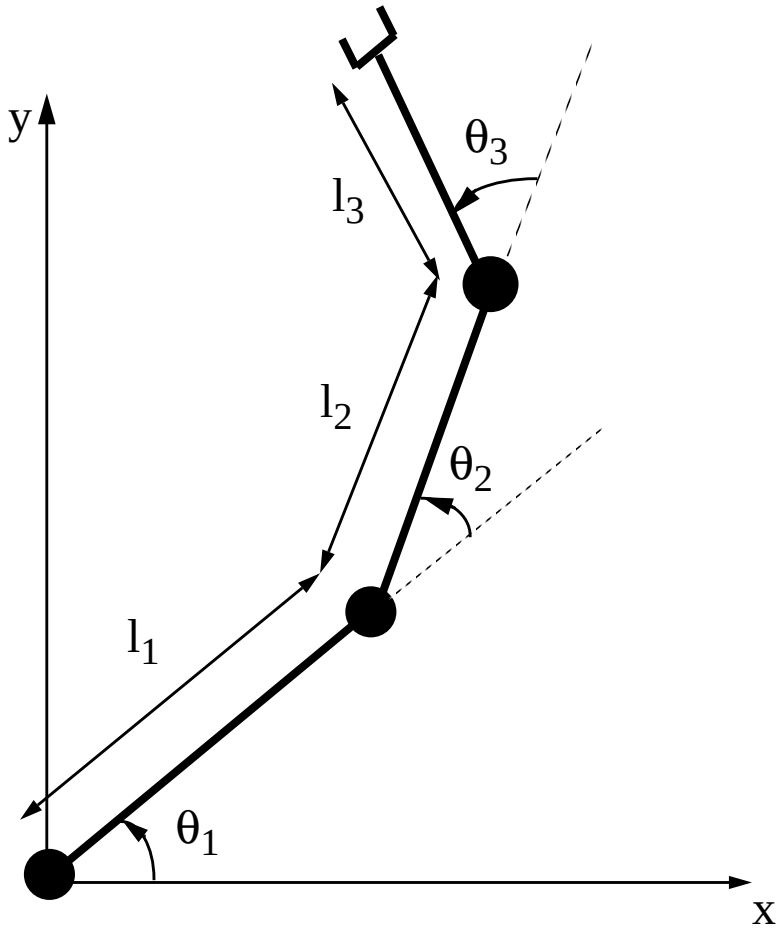


Figure 7: Three-link planar manipulator with rotary joints.

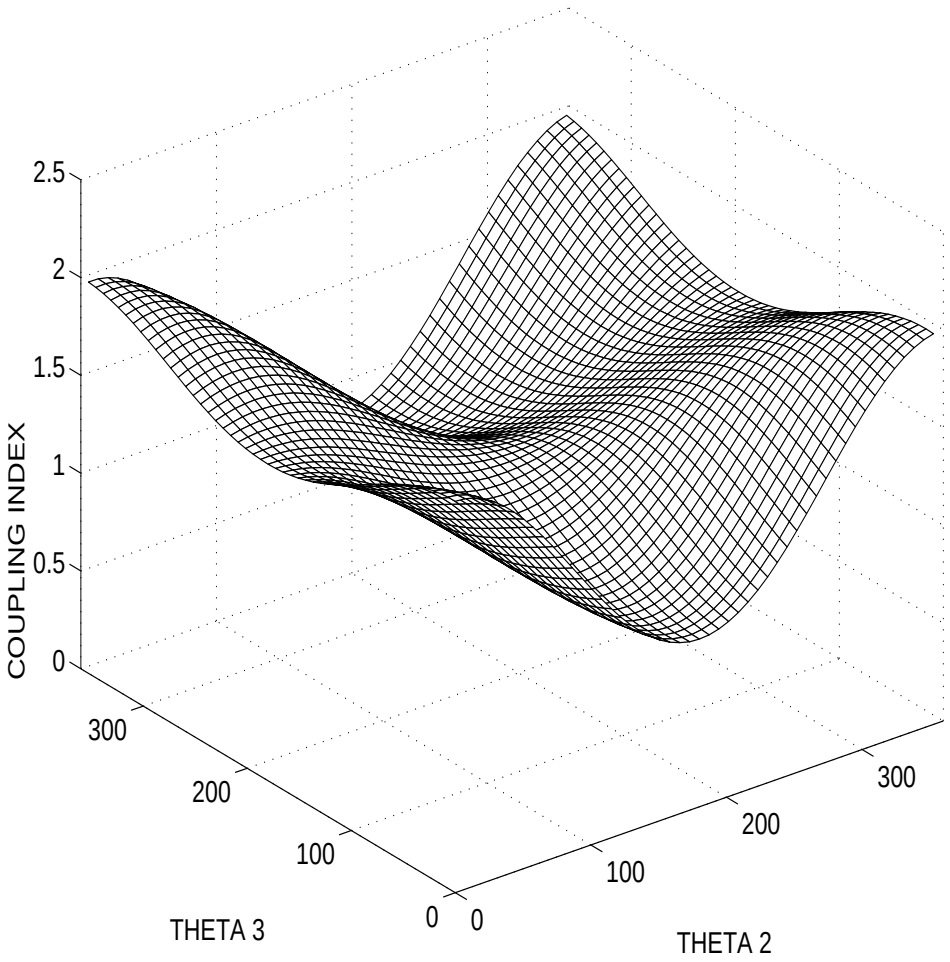


Figure 8: Coupling index for the manipulator in Figure 7, when joint 3 is passive.

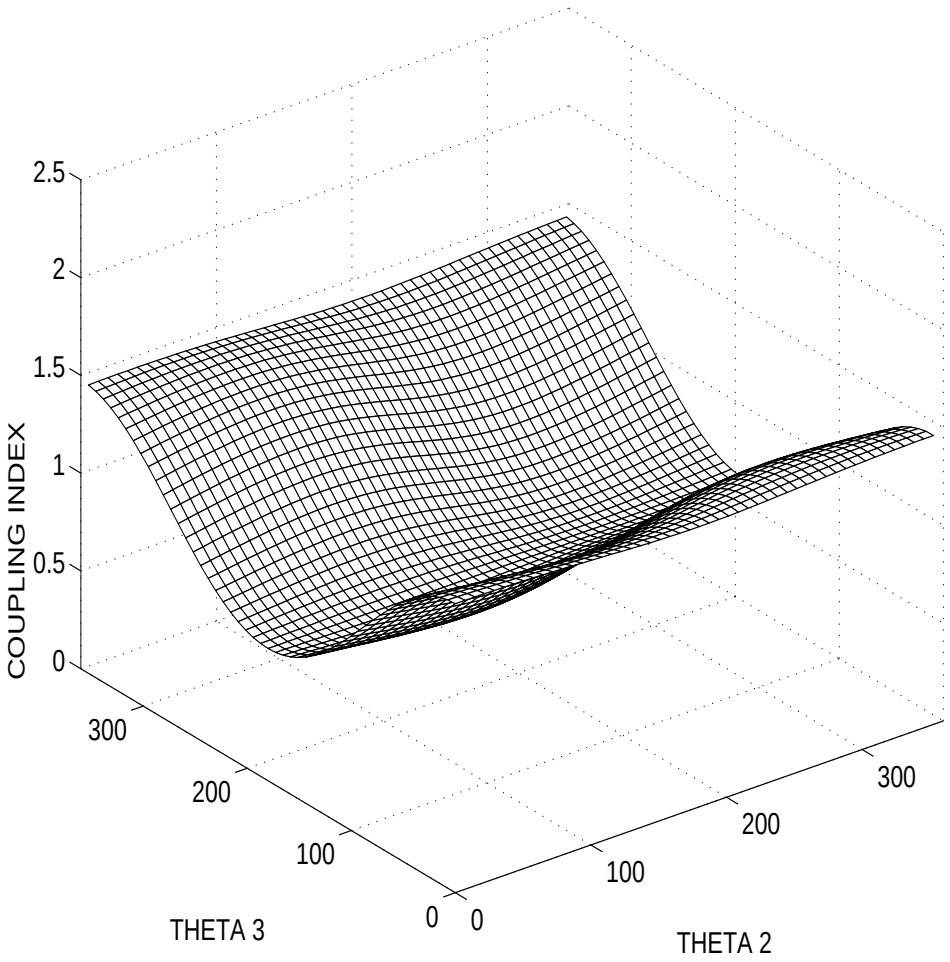


Figure 9: Coupling index for the manipulator in Figure 7, when joint 2 is passive.

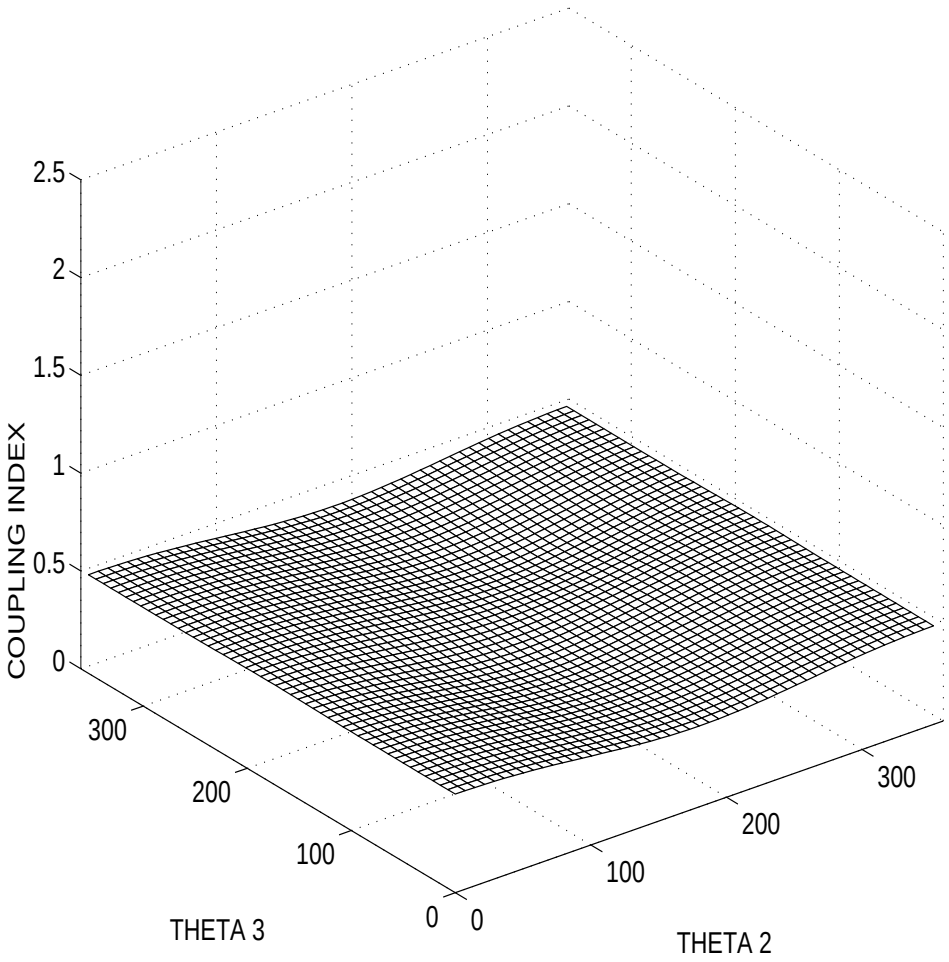


Figure 10: Coupling index for the manipulator in Figure 7, when joint 1 is passive.

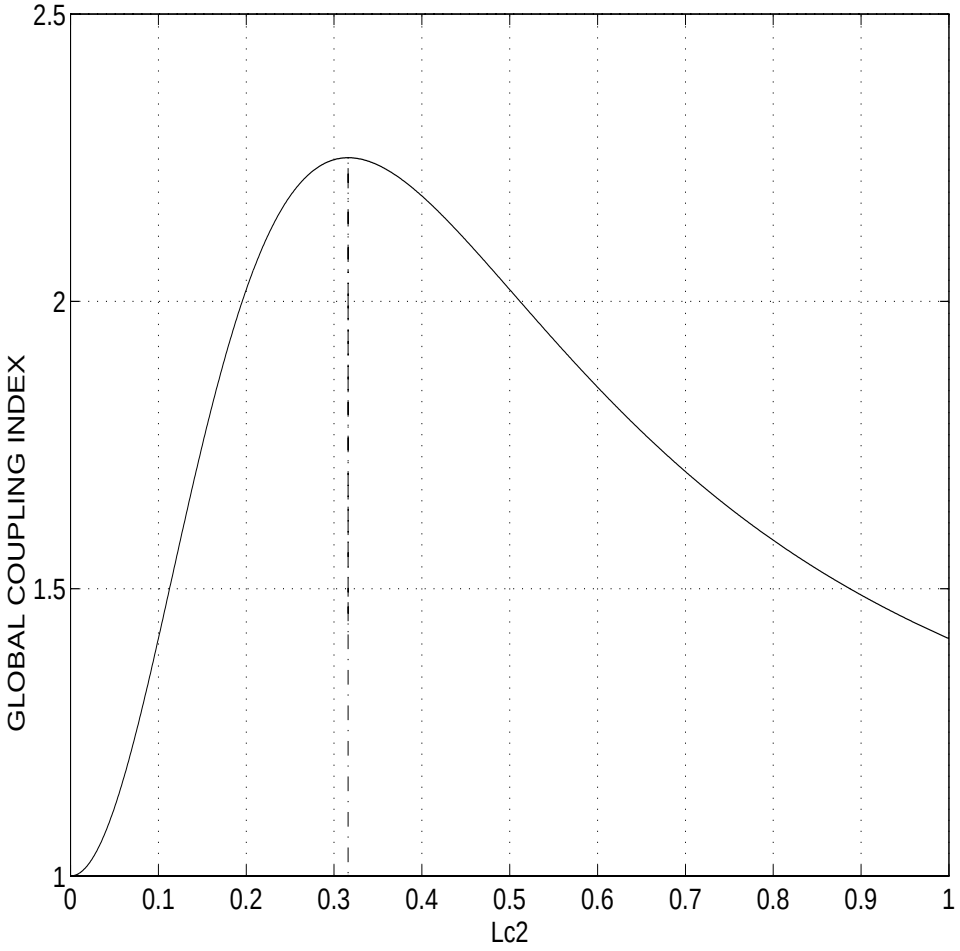


Figure 11: Global coupling index in example 10.

Table 1: Maximum, minimum, average and standard deviation values attained by ρ_{c_i}, $i = 1, 2, 3$.

i	$\max(\rho_{c_i})$	$\min(\rho_{c_i})$	$\text{avg}(\rho_{c_i})$	$\text{std}(\rho_{c_i})$
1	2.0021	0.8576	1.4211	0.3033
2	1.4774	0.6645	1.0607	0.2811
3	0.5104	0.3912	0.4556	0.0374

Table 2: Maximum, minimum, average and standard deviation values attained by $\rho_{c_{11}}$ and $\rho_{c_{12}}$.

i	$\max(\rho_{c_i})$	$\min(\rho_{c_i})$	$\text{avg}(\rho_{c_i})$	$\text{std}(\rho_{c_i})$
11	1.5454	0.4546	1.0000	0.2728
12	1.2727	0.7273	1.0000	0.1929

Table 3: Global coupling index $\rho^g_{c_i}$, $i = 1, 2, 3$.

i	$\rho^g_{c_i}$
1	2.1115
2	1.2041
3	0.2090

Table 4: Global individual joint coupling indices $\rho^g_{c_{11}}$ and $\rho^g_{c_{12}}$.

i	$\rho^g_{c_i}$
11	1.0372
12	1.0372